

Supplementary Materials

Core-shell nanostructures of graphene-wrapped CdS nanoparticles and TiO₂ (CdS@G@TiO₂): The role of graphene in enhanced photocatalytic H₂ generation

Muhammad Zubair¹, Ingeborg-Helene Svenum^{1,2}, Magnus Rønning¹ and Jia Yang^{1,*}

¹ Department of Chemical Engineering, Norwegian University of Science and Technology (NTNU), Sem Sælands vei 4, NO-7491, Trondheim, Norway;

muhammad.zubair@ntnu.no (M.Z.); svenum@ntnu.no (I.H.S.), magnus.ronning@ntnu.no (M.R.), jia.yang@ntnu.no (J.Y.)

² SINTEF Industry, P. O. Box 4760, Torgarden, NO-7465, Trondheim, Norway; ingeborg-helene.svenum@sintef.no (I.H.S.)

* Correspondence: jia.yang@ntnu.no; Tel.: +47-73593146

S1. Calculation steps for Apparent Quantum Efficiency (AQE):

Following well-known equations are used to calculate the AQE.

$$AQE = \frac{\text{Number of reacted electrons}}{\text{Total number of photons absorbed}} \times 100 \quad (1)$$

$$\text{Number of reacted electrons} = 2 \times [H_2] \times N_A \quad (2)$$

$$\text{Total number of photons absorbed} = \frac{\text{Light absorbed by the photocatalyst}}{\text{The energy of the photon}} \times t \quad (3)$$

$$\text{Light absorbed by the photocatalyst} = H \times A \quad (4)$$

$$\text{Energy of the photon} = hc/\lambda \quad (5)$$

- $[H_2] = 1510 \mu\text{mol}$ (by most active sample, i.e. CdS@50G@TiO₂)
- $N_A = 6.022 \times 10^{23} \text{ mol}^{-1}$
- $H = 1000 \text{ W m}^{-2}$ (intensity of 150W solar simulator at AM 1.5G conditions)
- $A = 0.0044 \text{ m}^2$ (linear surface area of the photoreactor illuminated during photocatalytic reaction)
- $h = 6.626 \times 10^{-34} \text{ J}$ (Planck's constant)
- $c = 3 \times 10^8 \text{ m s}^{-1}$ (speed of light)
- $\lambda = 393 \text{ nm}$ (average wavelength of broadband light source which is estimated with reference to the band gap of CdS (2.31 eV). The photons having less energy than the band gap of CdS will not excite the electron to the conduction band of CdS. Hence, the average wavelength of 250-536 nm is selected for AQE calculations [1–4].)

By combining the equations 1, 2, 3, 4 and 5, we obtained the values of AQE which are tabulated in Table S1.

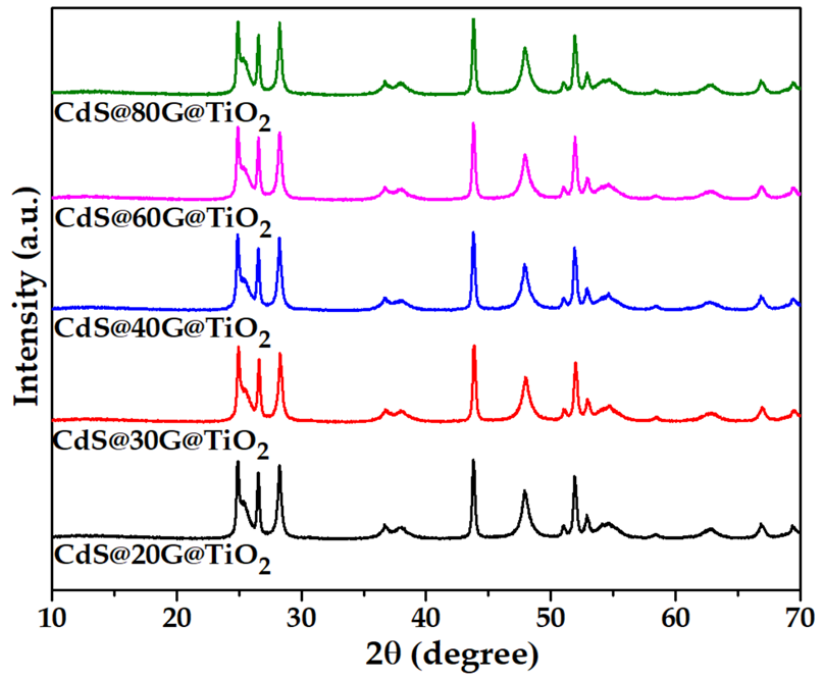


Figure S1. XRD pattern of CdS@xG@TiO₂ ($x = 20, 30, 40, 50, 60, 80$ μl of GQD solution with concentration of $\sim 100 \text{ mg mL}^{-1}$ were used in the synthesis).

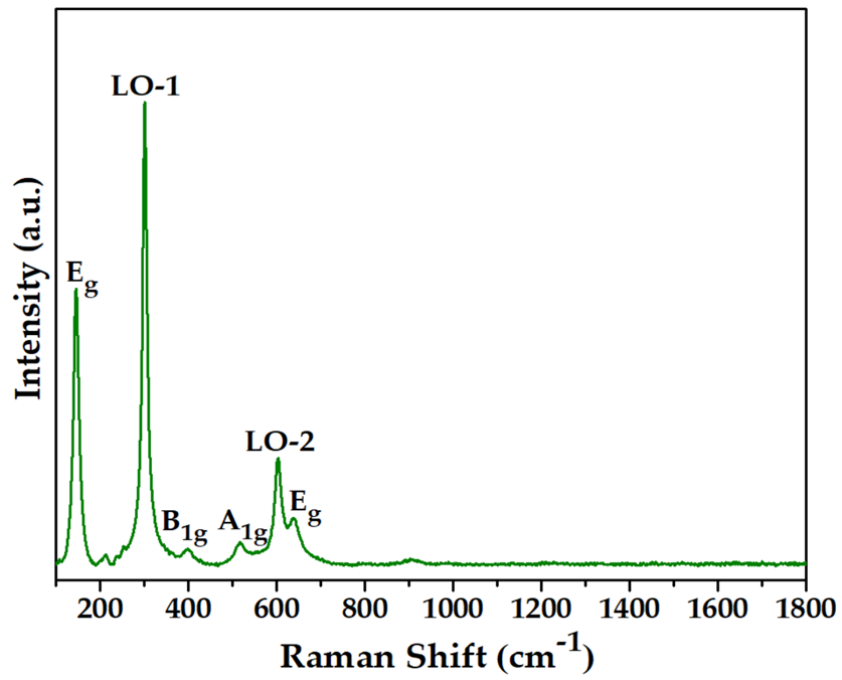


Figure S2. Raman spectrum of the CdS@50G@TiO₂ sample.

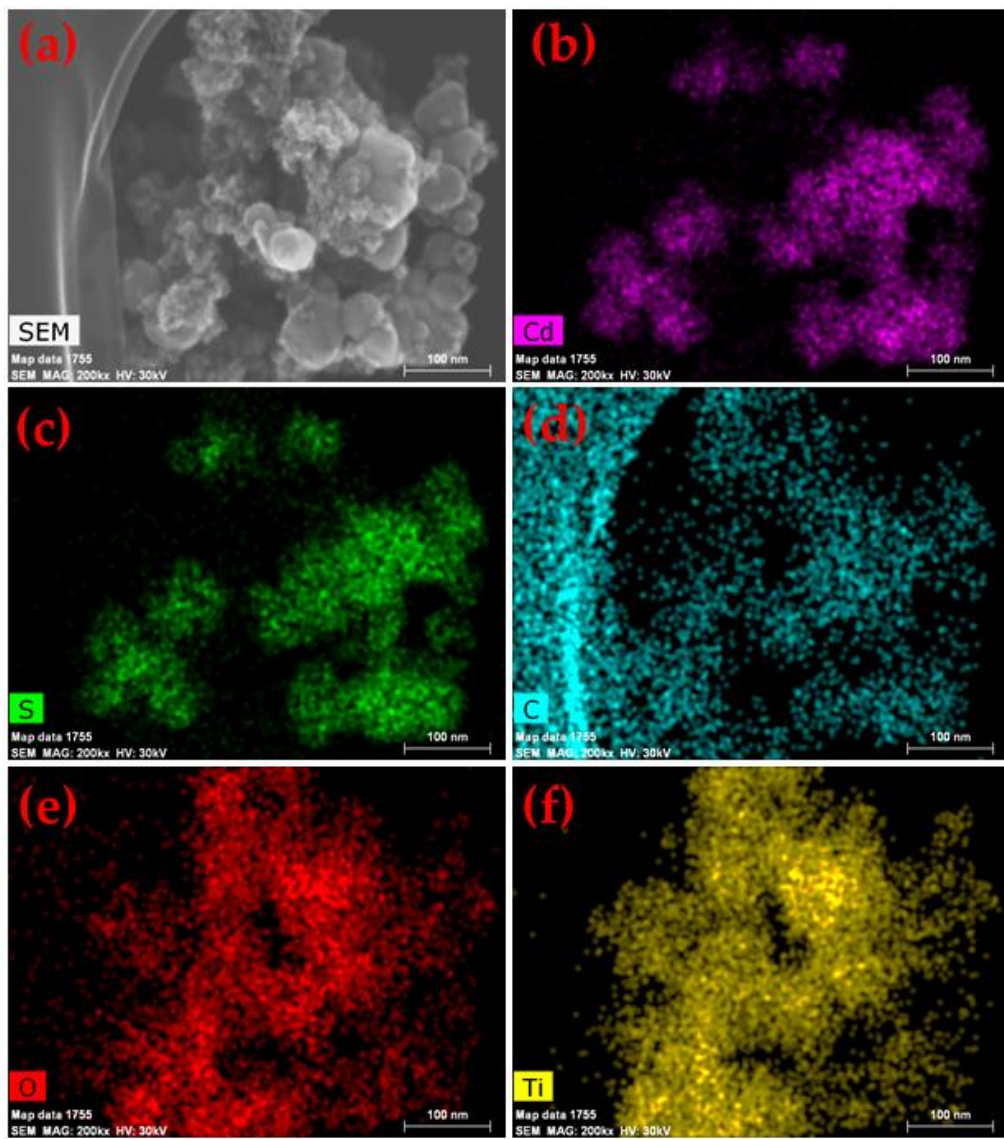


Figure S3. EDX elemental mapping images of the CdS@50G@TiO₂ sample which shows the presence of Cd, S, C, O and Ti in the sample.

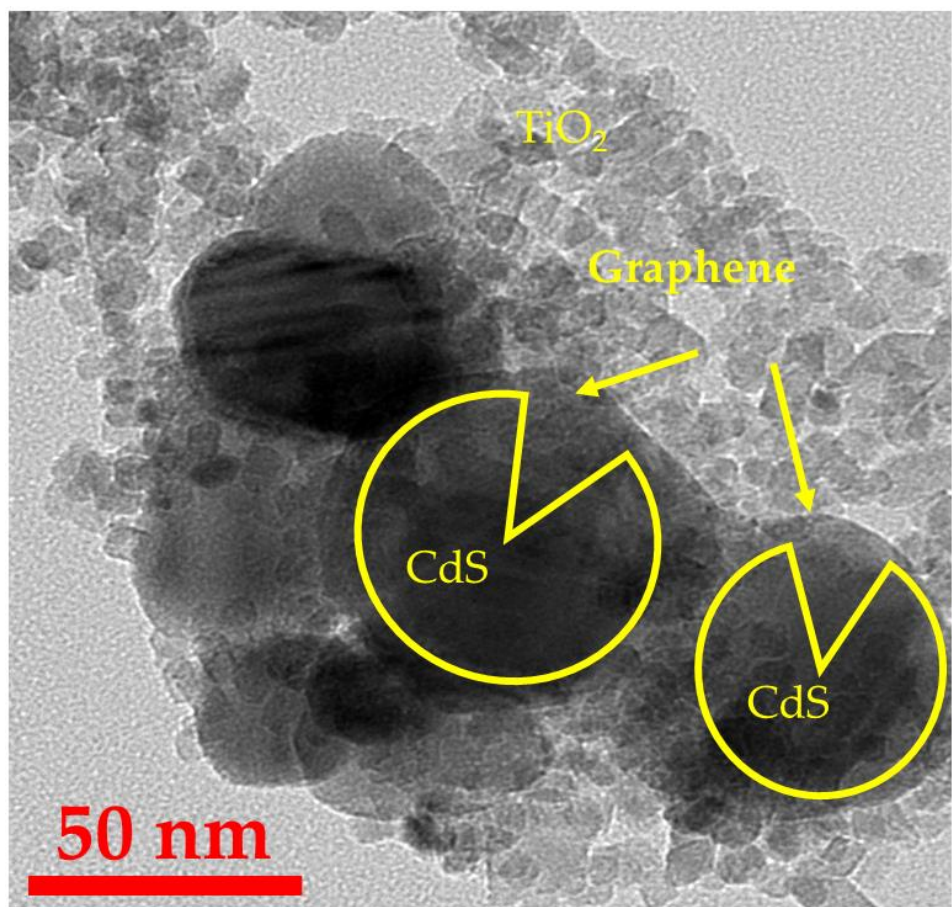


Figure S4. TEM image of the CdS@50G@TiO₂ sample.

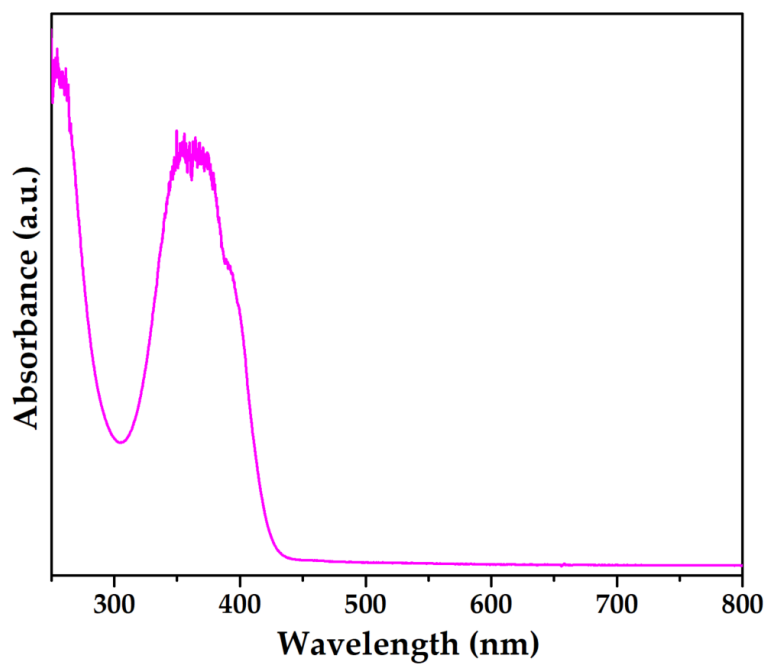


Figure S5. UV-vis spectrum of pure graphene quantum dots (GQD)

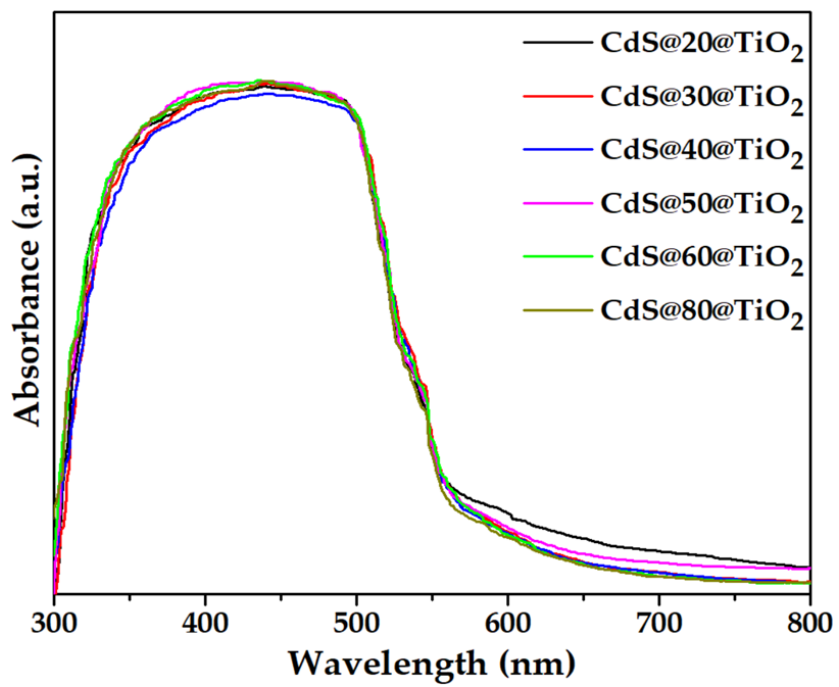


Figure S6. UV-vis DRS spectra of CdS@xG@TiO₂ samples.

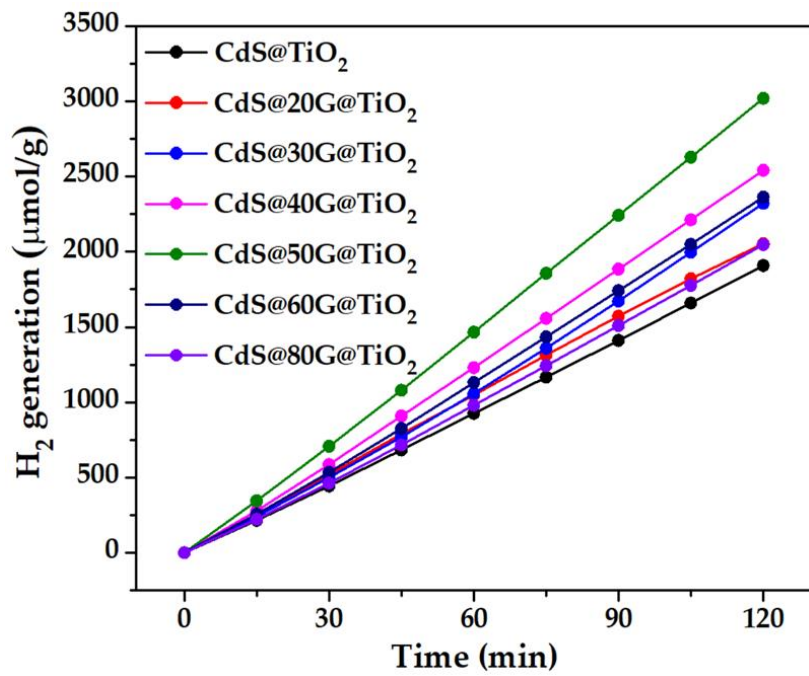


Figure S7. Photocatalytic H_2 generation from water employing CdS@TiO_2 and $\text{CdS}@x\text{G@TiO}_2$ samples under simulated solar light with 1.5 AM filter.

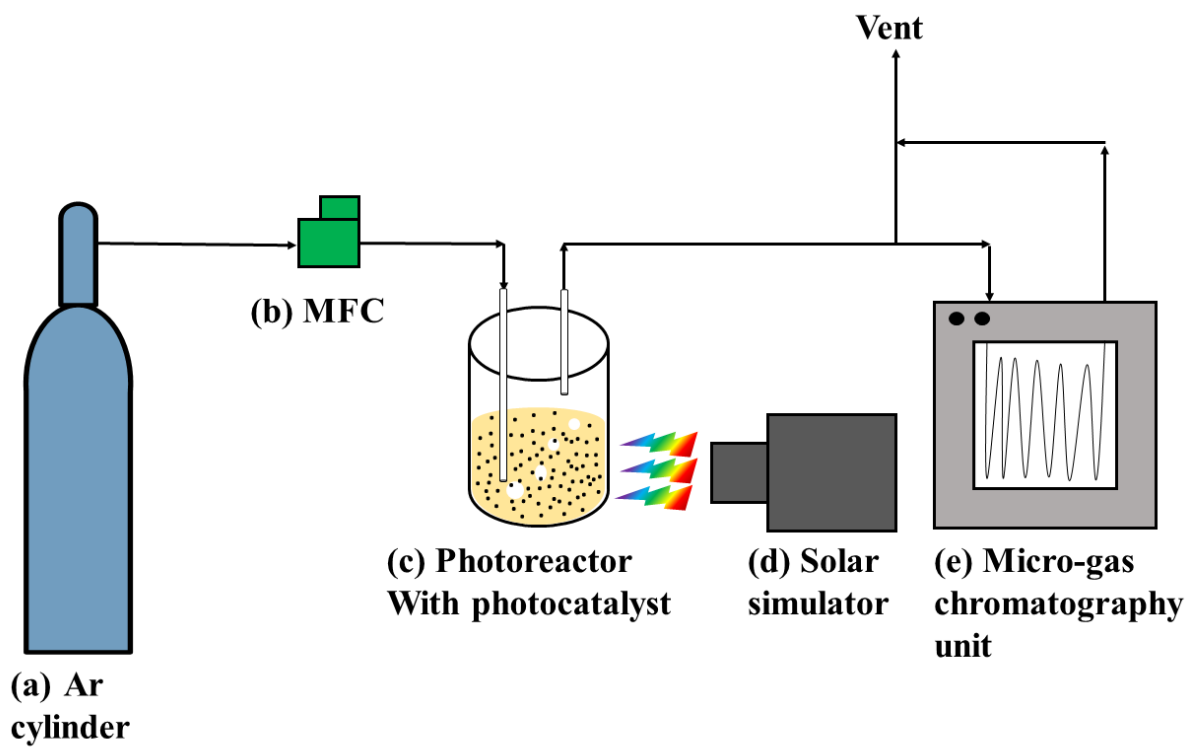


Figure S8. Schematic diagram of photocatalytic H₂ generation setup in which Ar gas (a) was bubbled through mass flow controller (b) from the photoreactor (c) ($V = 1.2\text{ L}$) filled with a uniform reaction mixture consisting of 40 mg photocatalyst in aqueous 0.125 M Na₂S and 0.175 M Na₂SO₃ solution. The photoreactor is illuminated with a solar simulator (d) equipped with AM 1.5 G filter and the effluent of the photoreactor is analyzed by a micro-gas chromatography unit (e).

Table S1. BET surface areas, H₂ production rates and apparent quantum efficiencies (AQE) of all the photocatalytic samples.

Sample	BET surface area m ² g ⁻¹	Hydrogen production μmol g ⁻¹ h ⁻¹	Apparent quantum efficiency %
Pure TiO ₂	375	565	2.16
Pure CdS	18	673	2.57
CdS@TiO ₂	110	954	3.65
CdS@20G@TiO ₂	97	1027	3.93
CdS@30G@TiO ₂	102	1160	4.45
CdS@40G@TiO ₂	107	1270	4.87
CdS@50G@TiO ₂	107	1510	5.78
CdS@60G@TiO ₂	110	1181	4.52
CdS@80G@TiO ₂	96	1024	3.92

Table S2. Comparison of various CdS-TiO₂ with carbon and noble metal based photocatalysts reported for photocatalytic H₂ generation from water.

Sr. Number	Photocatalyst sample	Light source	Reaction conditions	H ₂ generation	AQE
1	Pt/CdS/TiO ₂ [5]	Osram XBO 450W	Na ₂ S = 4.8 mM Na ₂ SO ₃ = 7.0 mM Mass of catalysts = 80 mg	0.9 μmol min ⁻¹	Not reported
2	Au@TiO ₂ -CdS [6]	300 W Xenon Lamp ($\lambda > 420$ nm)	Na ₂ S = 0.25 M Na ₂ SO ₃ = 0.35 M Mass of catalysts = 2 mg	3.94 μmol h ⁻¹	Not reported
3	C ₆₀ -Decorated CdS/TiO ₂ [7]	4 UV-LEDs (3 W, 420 nm)	Na ₂ S = 0.25 M Na ₂ SO ₃ = 0.25 M Mass of catalysts = 50 mg [Na ₂ S]:[Na ₂ SO ₃] = 0.1M	6.03 μmol h ⁻¹	2 %
4	Au@CdS/TiO ₂ [8]	300 W xenon arc lamp with a UV cutoff filter	Concentration of photocatalysts = 1g L ⁻¹ Na ₂ S = 0.02 M Na ₂ SO ₃ = 0.1 M	6.03 μmol After 3 hrs	Not reported
5	CdS-TiO ₂ [9]	500 W Tungsten filament bulb ($\lambda \leq 420$ nm)	Mass of catalysts = 50 mg Na ₂ S = 0.1 M Na ₂ SO ₃ = 0.1 M	0.86 mmol h ⁻¹ g ⁻¹	25.42 %
6	3DOM TiO ₂ -Au-CdS [10]	PLS-SXE-300C lamp	Mass of catalysts = 0.1 g Na ₂ S = 0.1 M Na ₂ SO ₃ = 0.1 M	0.18 mmol h ⁻¹ g ⁻¹ 1.81 mmol h ⁻¹ g ⁻¹	Not reported
7	1 wt% Pt-CdS-TiO ₂ [11]	450 W Hg-arc lamp	Mass of catalysts = 0.1 g Na ₂ SO ₃ = 0.02 M	3.94 μmol h ⁻¹	Not reported
8	Core-shell TiO ₂ -CdS [Our previous work] [4]	150 W Xenon solar simulator	Na ₂ S = 0.125 M Na ₂ SO ₃ = 0.175 M Mass of catalysts = 40 mg	954 μmol h ⁻¹ g ⁻¹	3.53%
9	CdS@G@TiO ₂ [current work]	150 W Xenon solar simulator	Na ₂ S = 0.125 M Na ₂ SO ₃ = 0.175 M Mass of catalysts = 40 mg	1510 μmol h ⁻¹ g ⁻¹	5.78%

Table S3. Comparison of various photocatalysts recently reported for photocatalytic H₂ generation from water.

Sr. Number	Photocatalyst sample	Light source	Reaction conditions	H ₂ generation	AQE
1	High crystalline 3% Pt-g-C ₃ N ₄ [12]	300W Xenon arc lamp	10 vol% triethanolamine Mass of catalysts = 50 mg	339 μmol h ⁻¹ g ⁻¹	Not reported
2	Pt/t-ZrO ₂ /g-C ₃ N ₄ [13]	300 W Xenon Lamp ($\lambda > 420$ nm)	10 vol% triethanolamine Mass of catalysts = 50 mg	722 μmol h ⁻¹ g ⁻¹	0.215 %
3	1 wt% Pt/DR-ZnS [14]	300 W Xenon Lamp ($\lambda > 420$ nm)	Na ₂ S = 0.1 M Na ₂ SO ₃ = 0.1 M Mass of catalysts = 20 mg 20% Methanol	70 μmol h ⁻¹	2.4 %
4	0.37 wt.% Pt- 2C-KNb ₃ O ₈ [15]	300 W Xe-lamp	Mass of catalysts = 50 mg	1148 μmol h ⁻¹ g ⁻¹	Not reported
5	3wt% WS ₂ /ZnIn ₂ S ₄ [16]	300 W Xe lamp ($\lambda \leq 420$ nm)	lactic acid Mass of catalysts = 30 mg	2.55 mmol h ⁻¹ g ⁻¹	3.2 %
6	ZnIn ₂ S ₄ /LaNiO ₃ [17]	300 W Xe lamp ($\lambda \leq 420$ nm)	TEOA Mass of catalysts = 20 mg	1600 μmol h ⁻¹ g ⁻¹	Not reported
7	Core-shell TiO ₂ -CdS [Our previous work] [4]	150 W Xenon solar simulator	Na ₂ S = 0.125 M Na ₂ SO ₃ = 0.175 M Mass of catalysts = 40 mg	954 μmol h ⁻¹ g ⁻¹	3.53%
8	CdS@G@TiO ₂ [current work]	150 W Xenon solar simulator	Na ₂ S = 0.125 M Na ₂ SO ₃ = 0.175 M Mass of catalysts = 40 mg	1510 μmol h ⁻¹ g ⁻¹	5.78%

Table. S4. Estimated values of valence band potential (E_{VB}), conduction band potential (E_{CB}) bandgap (E_g) and difference in the valance band potential (ΔE_{VB}) for pure CdS and pure TiO₂ nanoparticles. The valence band maximum (E_{VBM}) measured by valance band XPS.

Sample	E_{VB} (eV)	E_{CB} (eV)	E_g (eV)	ΔE_{VB} (eV)	E_{VBM} (eV)	ΔE_{VBM} (eV)
Pure CdS	2.00	-0.31	2.31		1.6	
				0.95		0.9
Pure TiO ₂	2.95	-0.05	3.0		2.5	

References

1. Ong, W.-J.; Tan, L.-L.; Chai, S.-P.; Yong, S.-T.; Mohamed, A.R. Surface charge modification via protonation of graphitic carbon nitride (g-C₃N₄) for electrostatic self-assembly construction of 2D/2D reduced graphene oxide (rGO)/g-C₃N₄ nanostructures toward enhanced photocatalytic reduction of carbon dioxide to methane. *Nano Energy* **2015**, *13*, 757–770.
2. Liu, L.; Jiang, Y.; Zhao, H.; Chen, J.; Cheng, J.; Yang, K.; Li, Y. Engineering Coexposed {001} and {101} Facets in Oxygen-Deficient TiO₂ Nanocrystals for Enhanced CO₂ Photoreduction under Visible Light. *ACS Catal.* **2016**, *6*, 1097–1108.
3. Zubair, M.; Razzaq, A.; Grimes, C.A.; In, S. Il Cu₂ZnSnS₄(CZTS)-ZnO: A noble metal-free hybrid Z-scheme photocatalyst for enhanced solar-spectrum photocatalytic conversion of CO₂to CH₄. *J. CO₂ Util.* **2017**, *20*, 301–311.
4. Zubair, M.; Svenum, I.-H.; Rønning, M.; Yang, J. Facile synthesis approach for core-shell TiO₂–CdS nanoparticles for enhanced photocatalytic H₂ generation from water. *Catal. Today* **2019**, *328*, 15–20.
5. Daskalaki, V.M.; Antoniadou, M.; Li Puma, G.; Kondarides, D.I.; Lianos, P. Solar Light-Responsive Pt/CdS/TiO₂ Photocatalysts for Hydrogen Production and Simultaneous Degradation of Inorganic or Organic Sacrificial Agents in Wastewater. *Environ. Sci. Technol.* **2010**, *44*, 7200–7205.
6. Fang, J.; Xu, L.; Zhang, Z.; Yuan, Y.; Cao, S.; Wang, Z.; Yin, L.; Liao, Y.; Xue, C. Au@TiO₂–CdS Ternary Nanostructures for Efficient Visible-Light-Driven Hydrogen Generation. *ACS Appl. Mater. Interfaces* **2013**, *5*, 8088–8092.
7. Lian, Z.; Xu, P.; Wang, W.; Zhang, D.; Xiao, S.; Li, X.; Li, G. C 60 -Decorated CdS/TiO₂ Mesoporous Architectures with Enhanced Photostability and Photocatalytic Activity for H₂ Evolution. *ACS Appl. Mater. Interfaces* **2015**, *7*, 4533–4540.
8. Kim, M.; Kim, Y.K.; Lim, S.K.; Kim, S.; In, S.-I. Efficient visible light-induced H₂ production by Au@CdS/TiO₂ nanofibers: Synergistic effect of core–shell structured Au@CdS and densely packed TiO₂ nanoparticles. *Appl. Catal. B Environ.* **2015**, *166–167*, 423–431.
9. Oskoui, M.S.; Khatamian, M.; Haghghi, M.; Yavari, A. Photocatalytic hydrogen evolution from water over chromosilicate-based catalysts. *RSC Adv.* **2014**, *4*, 19569.
10. Zhao, H.; Wu, M.; Liu, J.; Deng, Z.; Li, Y.; Su, B.-L. Synergistic promotion of solar-driven H₂ generation by three-dimensionally ordered macroporous structured TiO₂ –Au-CdS ternary photocatalyst. *Appl. Catal. B Environ.* **2016**, *184*, 182–190.
11. JANG, J.; KIM, H.; JOSHI, U.; JANG, J.; LEE, J. Fabrication of CdS nanowires decorated with TiO₂ nanoparticles for photocatalytic hydrogen production under visible light irradiation. *Int. J. Hydrogen Energy* **2008**, *33*, 5975–5980.
12. Wang, L.; Hong, Y.; Liu, E.; Wang, Z.; Chen, J.; Yang, S.; Wang, J.; Lin, X.; Shi, J. Rapid polymerization synthesizing high-crystalline g-C₃N₄ towards boosting solar photocatalytic H₂ generation. *Int. J. Hydrogen Energy* **2020**, *45*, 6425–6436.
13. Li, H.; Wu, Y.; Li, C.; Gong, Y.; Niu, L.; Liu, X.; Jiang, Q.; Sun, C.; Xu, S. Design of Pt/t-ZrO₂/g-C₃N₄ efficient photocatalyst for the hydrogen evolution reaction. *Appl.*

Catal. B Environ. **2019**, *251*, 305–312.

14. Zhu, S.; Qian, X.; Lan, D.; Yu, Z.; Wang, X.; Su, W. Accelerating charge transfer for highly efficient visible-light-driven photocatalytic H₂ production: In-situ constructing Schottky junction via anchoring Ni-P alloy onto defect-rich ZnS. *Appl. Catal. B Environ.* **2020**, *269*, 118806.
15. He, Y.; Dai, X.; Ma, S.; Chen, L.; Feng, Z.; Xing, P.; Yu, J.; Wu, Y. Hydrothermal preparation of carbon modified KNb₃O₈ nanosheets for efficient photocatalytic H₂ evolution. *Ceram. Int.* **2020**.
16. Xiong, M.; Chai, B.; Yan, J.; Fan, G.; Song, G. Few-layer WS₂ decorating ZnIn₂S₄ with markedly promoted charge separation and photocatalytic H₂ evolution activity. *Appl. Surf. Sci.* **2020**, *514*, 145965.
17. Wang, Z.; Su, B.; Xu, J.; Hou, Y.; Ding, Z. Direct Z-scheme ZnIn₂S₄/LaNiO₃ nanohybrid with enhanced photocatalytic performance for H₂ evolution. *Int. J. Hydrogen Energy* **2020**, *45*, 4113–4121.